Direct Dynamics Simulation of the Lifetime of Trimethylene

Charles Doubleday, Jr.,*,† Kim Bolton,‡ Gilles H. Peslherbe,§ and William L. Hase*,‡

Contribution from the Departments of Chemistry, Columbia University, New York, New York 10027, and Wayne State University, Detroit, Michigan 48202

Received July 15, 1996. Revised Manuscript Received August 16, 1996[⊗]

Abstract: A direct trajectory method was employed to investigate the intramolecular dynamics and unimolecular decay of the trimethylene biradical over a range of energies. This method proved to be computationally viable when the internuclear forces were determined by semiempirical molecular orbital theory. The trimethylene decay is double exponential at low energies, but becomes single exponential with a statistical rate constant as the energy is increased. The non-statistical behavior at low energies arises from incomplete intramolecular vibrational energy redistribution (IVR). The simulated results are in good agreement with the available experimental data.

I. Introduction

A fundamental goal of chemical dynamics is to obtain a microscopic picture of how energy flows and atoms move during the course of a chemical reaction.[1,2] Both theoretical and chemical approaches have focused on this goal and their use, in complementary ways, has often proven particularly effective.[3] Classical trajectory[4] and time-dependent quantum[5] calculations give a complete picture of the reaction event. Recently it has become possible to obtain the same level of detail from real-time laser femtochemistry experiments,[6] in which one "observes" the motion of the atoms involved in the chemical reaction.

The microscopic mechanism of the unimolecular decay of cyclopropane and cyclobutane has intrigued chemists for more than 50 years. Of particular interest are the possible roles the trimethylene and tetramethylene biradicals play in these reactions, and understanding them is a central issue in developing accurate models for chemical kinetics and dynamics. Quantum chemical calculations of potential energy surface (PES) properties have helped characterize these biradicals as transition states or reaction intermediates. Recently Pedersen, Herek, and Zewail used laser femtochemistry to observe them and measure their lifetimes.[7] Following this work, Doubleday calculated a trimethylene PES from a high level complete active space multiconfiguration self-consistent field (CASSCF)[8] *ab initio* calculation and used it in a variational RRKM[9−11] calculation of the trimethylene lifetime.[12] Though the experimental lifetime is fairly short, *i.e.*, 120 ± 20 fs,[7] and RRKM theory assumes that energy is randomized among all the biradical degrees of freedom, the RRKM lifetime is in near exact agreement with that determined experimentally.

In this paper classical trajectory simulations of the intramolecular and unimolecular behavior of the trimethylene biradical are reported. These calculations provide further insight into the experiments of Zewail's group and test the RRKM model used by Doubleday. A previous trajectory study[13] involving the trimethylene radical was based on a reduced dimension analytic potential energy function derived from quantum chemical calculations. The focus of the work presented here is exclusively on the trimethylene lifetime and not with the question of double and single methylene rotations in trimethylene.

Here a direct dynamics simulation[14−21] is used in which trajectories are integrated "on the fly", without an analytic potential, by obtaining the energy and gradient directly from electronic structure theory. For short time events *ab initio* direct dynamics is possible.[15,17,18] However, this approach is not practical for following the long-time (*i.e.*, picosecond) dynamics of the trimethylene biradical and, instead, semiempirical direct dynamics is employed.[14,16,19−21] The trajectories are calculated by interfacing the general dynamics computer program VENUS[22] with the semiempirical electronic structure theory package MOPAC 7.0.[23] The resulting program is called

† Columbia University.
‡ Wayne State University.
§ Present address: Department of Chemistry and Biochemistry, University of Colorado at Boulder, Boulder, CO 80309-0215.
⊗ Abstract published in *Advance ACS Abstracts,* October 1, 1996.

(1) Levine, R. D.; Bernstein, R. B. *Molecular Reaction Dynamics and Chemical Reactivity*; Oxford: New York, 1987.
(2) Steinfeld, J. I.; Francisco, J. S.; Hase, W. L. *Chemical Kinetics and Dynamics*; Prentice Hall: Englewood Cliffs, NJ, 1989.
(3) Hase, W. L. *Science* **1994**, *266*, 998.
(4) Bunker, D. L. *Sci. Am.* **1969**, *211*, 100.
(5) Heller, E. J. *J. Chem. Phys.* **1975**, *62*, 1544. Kosloff, R.; Kosloff, D. *J. Chem. Phys.* **1983**, *79*, 1823.
(6) Zewail, A. H. *Femtochemistry: Ultrafast Dynamics of the Chemical Bond*; World Scientific: Singapore, 1994.
(7) Pedersen, S.; Herek, J. L.; Zewail, A. H. *Science* **1994**, *266*, 1359.
(8) Roos, B.; Taylor, P.; Siegbahn, P. *Chem. Phys.* **1980**, *48*, 157. Ruedenberg, K.; Schmidt, M. W.; Gilbert, M. M.; Elbert, S. T. *Chem. Phys.* **1982**, *71*, 41. Lengsfield, B., III *J. Chem. Phys.* **1982**, *77*, 4073.
(9) Garrett, B. C.; Truhlar, D. G. *J. Chem. Phys.* **1979**, *70*, 1593.
(10) Truhlar, D. G. *J. Phys. Chem.* **1979**, *83*, 188.
(11) Hase, W. L. *J. Chem. Phys.* **1972**, *57*, 730. Hase, W. L. *Acc. Chem. Res.* **1983**, *16*, 258. Wardlaw, D. M.; Marcus, R. A. *Adv. Chem. Phys.* **1988**, *70*, 231.
(12) Doubleday, D., Jr *J. Phys. Chem.* **1996**, *100*, 3520.
(13) Jean, Y.; Chapuisat, X. *J. Am. Chem. Soc.* **1974**, *96*, 6911. Chapuisat, X.; Jean, Y. *J. Am. Chem. Soc.* **1975**, *97*, 6325.
(14) Wang, I. S. Y.; Karplus, M. *J. Am. Chem. Soc.* **1973**, *95*, 8160.
(15) LeForestier, C. *J. Chem. Phys.* **1978**, *68*, 4406.
(16) Truhlar, D. G.; Duff, J. W.; Blais, N. C.; Tully, J. C.; Garrett, B. C. *J. Chem. Phys.* **1982**, *77*, 764.
(17) Helgaker, T.; Uggerud, E.; Jensen, H. *Chem. Phys. Lett.* **1990**, *173*, 145. Uggerud, E.; Helgaker, T. *J. Am. Chem. Soc.* **1992**, *114*, 4265.
(18) Chen, W.; Hase, W. L.; Schlegel, H. B. *Chem. Phys. Lett.* **1994**, *228*, 436.
(19) Carmer, C. S.; Weiner, B.; Frenklach, M. *J. Chem. Phys.* **1993**, *99*, 1356. Zhao, X. G.; Carmer, C. S.; Weiner, B.; Frenklach, M. *J. Phys. Chem.* **1993**, *97*, 1639.
(20) Peslherbe, G. H.; Wang, H.; Hase, W. L. *J. Am. Chem. Soc.* **1996**, *118*, 2257.
(21) Peslherbe, G. H.; Hase, W. L. *J. Chem. Phys.* **1996**, *104*, 7882.
(22) Hase, W. L.; Duckovic, R. J.; Hu, X.; Lim, K.; Lu, D.-h; Peslherbe, G. H.; Swamy, K. N.; Vande Linde, S. R.; Wang, H.; Wolfe, R. J. VENUS, a General Chemical Dynamics Computer Program. To be submitted to QCPE. Venus is an enhanced version of MERCURY: Hase, W. L. *QCPE* **1983**, *3*, 453.

S0002-7863(96)02434-1 CCC: $12.00

VENUS-MOPAC.[24] The AM1 parameters[25] in MOPAC, supplemented with specific reaction parameters[26] (SRPs), are used in the trimethylene direct dynamics.

Semiempirical direct dynamics with SRPs has been used in two recent studies[20,21] with mixed results. For formaldehyde dissociation to $H_2 + CO$ this approach was unable to reproduce the experimental product energy partitioning or that determined by *ab initio* direct dynamics, even with SRPs chosen to reproduce the *ab initio* PES.[21] On the other hand, the *ab initio* direct dynamics results were in excellent agreement with experiment.[18] Apparently the semiempirical-SRP model cannot represent the subtle PES features which influence product energy partitioning for formaldehyde dissociation. More success was obtained when using AM1-SRP direct dynamics to study the intramolecular and unimolecular dynamics of the $Cl^- - CH_3Br$ complex.[20] The AM1-SRP calculation gave non-RRKM dynamics as found in a classical trajectory study based on an analytic PES derived by fitting *ab initio* calculations and experimental data. However, detailed aspects of the $Cl^- - CH_3$-Br dynamics determined from the AM1-SRP model were strikingly different from those found from the analytic surface. The simulations reported here for trimethylene and their comparison with the experiments of Zewail's group provide another test of the AM1-SRP direct dynamics model.

II. AM1-SRP Semiempirical Model

The goal in constructing the PES was to mimic essential features of the *ab initio* surface[12,27] and to reproduce the experimental activation energies of cyclopropane isomerizations.[28] We used the AM1 Hamiltonian[25] in the MOPAC 7.0[23] semiempirical package modified by the use of specific reaction parameters.[26] The resulting model is designated as AM1-SRP. Use of the BIRADICAL keyword, which invokes a 3×3 CI including $HOMO^2$, $HOMO^1LUMO^1$, and $LUMO^2$ obtained by the half-electron method,[29] gave a qualitatively reasonable description of trimethylene and the cyclization process. The H-transfer saddle point required a 4-electron-4-orbital treatment in the CASSCF *ab initio* treatment.[12] In MOPAC, as expected, use of 3×3 CI gave an unacceptably high barrier for H-transfer. However, the 3×3 CI wave function was found to give reasonable results for both cyclization and H-transfer if the 2-center 1-electron (resonance) integrals of AM1 were multiplied by a different parameter for each of 5 atomic pairs. For atomic orbitals μ,ν located on different atoms, the original resonance integral $H_{\mu\nu}$ was changed to $H'_{\mu\nu} = \beta_{\mu\nu}H_{\mu\nu}$, where $\beta_{\mu\nu}$ depended only on μ and ν. To lower the barrier to H-transfer the resonance integrals involving the middle hydrogens H_3, H_4 (see Figure 1) and the terminal carbons C_1, C_3 were increased. The resulting scale parameters are $\beta_{H_3C_1s} = \beta_{H_4C_1s} = \beta_{H_3C_3s} = \beta_{H_4C_3s} = 1.20$ and $\beta_{H_3C_1p} = \beta_{H_4C_1p} = \beta_{H_3C_3p} = \beta_{H_4C_3p} = 1.25$. Parameters were also needed for cyclization since the unmodified reaction was only 30 kcal mol^{-1} exothermic and the cyclization saddle point occurred much later than on the *ab initio* surface. Therefore the resonance integrals between the terminal carbons were increased with $\beta_{C_1sC_3s} = \beta_{C_1sC_3p} = \beta_{C_1pC_3s} = \beta_{C_1pC_3p} = 1.20$.

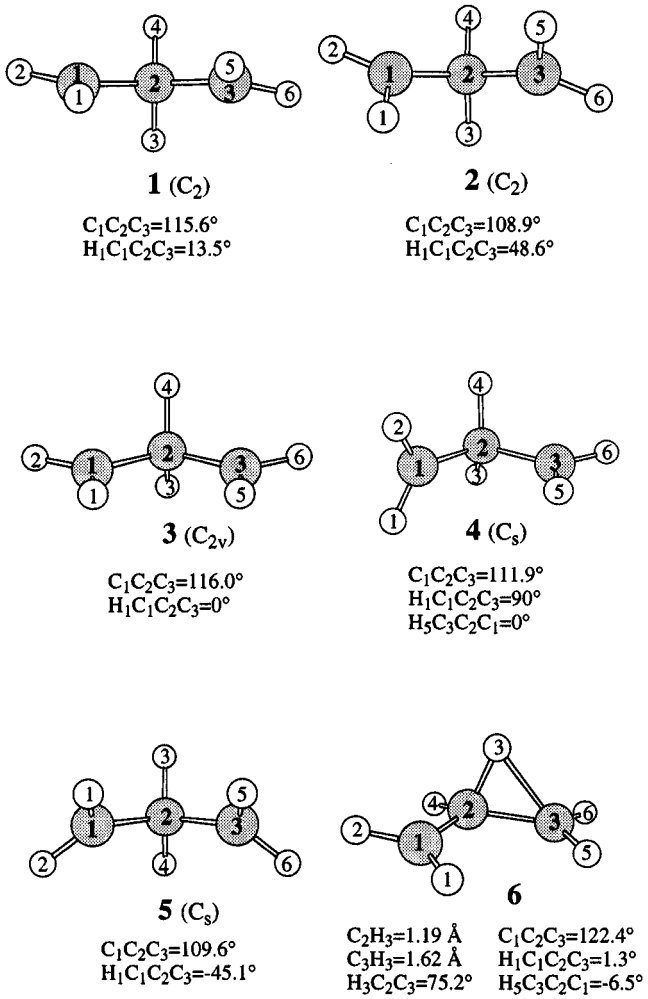

Figure 1. Stationary point structures obtained from the AM1-SRP Hamiltonian.

As a result of these changes the biradical region of the PES bore a close resemblance to the *ab initio* surface in most respects, but the increased resonance integrals made the products about 30 kcal mol^{-1} too exothermic. The exothermicities were adjusted by adding five potential energy terms V_α where

$$V_\alpha(r_\alpha) = D_\alpha[1 - (1 - e^{-c_\alpha(r_\alpha - r_\alpha^0)})^2]S_\alpha(r_\alpha), \quad r_\alpha > r_\alpha^0$$
$$= D_\alpha, \quad r_\alpha \le r_\alpha^0 \tag{1}$$

and

$$S_\alpha(r_\alpha) = {}^1/_2[1 + \tanh(g_\alpha(h_\alpha - r_\alpha))] \tag{2}$$

The index α is C_1C_3 for cyclization and $\alpha = C_1H_3$, C_1H_4, C_3H_3, C_3H_4 for the four possible H-transfers. The V_α are in the form of an inverted Morse potential multiplied by a switching function S_α which varies from 0 to 1 such that the energy correction is turned on as the products are approached, but there is no effect in the biradical region of the PES. Since the products are

(23) Stewart, J. P. P. MOPAC 7.0, a General Molecular Orbital Package. *QCPE* **1993**, 455. Stewart, J. P. P. *J. Comput. Chem.* **1989**, *10*, 209.

(24) Peslherbe, G. H.; Hase, W. L. VENUS-MOPAC, a General Chemical Dynamics and Semiempirical Direct Dynamics Computer Program. To be released.

(25) Dewar, M. J. S.; Zoebisch, E. G.; Healy, E. F.; Stewart, J. J. P. *J. Am. Chem. Soc.* **1985**, *107*, 3902.

(26) Variational TST calculations using MOPAC with specific reaction path parameters have been reported in: Gonzalez-Lafont, A.; Truong, T. N.; Truhlar, D. G. *J. Phys. Chem.* **1991**, *95*, 4618. Liu, Y.-P.; Lu, D.-h.; Gonzalez-Lafont, A.; Truhlar, D. G.; Garrett, B. C. *J. Am. Chem. Soc.* **1993**, *115*, 7806.

(27) Yamaguchi, Y.; Schaefer, H. F., III; Baldwin, J. E. *Chem. Phys. Lett.* **1991**, *185*, 143. Baldwin, J. E.; Yamaguchi, Y.; Schaefer, H. F., III *J. Phys. Chem.* **1994**, *98*, 7513. Getty, S. J.; Davidson, E. R.; Borden, W. T. *J. Am. Chem. Soc.* **1992**, *114*, 2085.

(28) Schlag, E. W.; Rabinovitch, B. S. *J. Am. Chem. Soc.* **1960**, *82*, 5996. Waage, E. V.; Rabinovitch, B. S. *J. Phys. Chem.* **1972**, *76*, 1965. Rabinovitch, B. S. *Chem. Phys.* **1982**, *67*, 201.

(29) Dewar, M. J. S.; Hashmall, J. A.; Venier, C. G. *J. Am. Chem. Soc.* **1968**, *90*, 1953. Dewar, M. J. S.; Trinajstic, N. *J. Chem. Soc. A* **1971**, 1220.

Table 1. Trimethylene Stationary Points Located with *ab Initio* and AM1-SRP Wave Functions

	ab initio[a]		AM1-SRP				
stationary point	sym	E_{rel}[b]	sym	E_{rel}[b]	ZPE[c]	E_{rel} + ZPE[d]	$\nu^{\ddagger}$ [e]
C_2 minimum (con) **1**	C_2	0.0	C_2	0.0	47.4	0.0	
C_2 cycl. saddle point (con) **2**	C_2	−0.1	C_2	0.4	47.4	0.4	204*i*
C_s minimum (dis)	C_s	0.5					
C_s cycl. saddle point (dis) **5**	C_s	1.2	C_s	2.8	47.2	2.6	322*i*, 135*i*[f]
Con-Dis saddle point[g]	C_1	0.3					
Con-Con saddle point **3**			C_{2v}	0.01	47.3	−0.1	42*i*
CH_2 twist saddle point **4**	C_1	1.9	C_s	2.0	47.2	1.8	231*i*
H-transfer saddle point **6**	C_1	7.9	C_1	7.4	46.8	6.8	1310*i*
cyclopropane			C_{2v}[h]	−61.6	51.2	−57.8	
propylene			C_s	−68.6	48.7	−67.3	

[a] MRCI energies from ref 12. [b] Energy relative to C_2 minimum in kcal mol^{-1}, excluding zero point energy. [c] Zero point vibrational energy, kcal mol^{-1}. [d] Energy relative to C_2 minimum in kcal mol^{-1}, including zero point energy. [e] Imaginary frequency of saddle point, cm^{-1}. [f] Has two negative eigenvalues of the second derivative matrix. [g] Saddle point for interconversion of C_2 and C_s minima. [h] AM1-SRP parameters have the symmetry of trimethylene, not D_{3h} cyclopropane.

mutually exclusive, at most one of the five V_α is appreciably different from zero at any given time. In eq 1 r_α ($\alpha = C_iH_j$) is the bond length of the nascent C_i-H_j bond during H-transfer, r_α ($\alpha = C_1C_3$) is the C_1-C_3 distance during cyclization, r_α^0 is an effective bond length, D_α is the maximum energy correction applied at $r_\alpha \le r_\alpha^0$, c_α controls the sharpness of the Morse potential, g_α controls the rate at which the switching function is turned on, and h_α is the point at which the switching function is turned on half way. The values were $D_{C_iH_j} = 37$ kcal mol^{-1}, $D_{C_1C_3} = 28$ kcal mol^{-1}, $c_{C_iH_j} = c_{C_1C_3} = 4.5$ Å^{-1}, $r^0_{C_iH_j} = 1.045$ Å, $r^0_{C_1C_3} = 1.42$ Å, $g_{C_iH_j} = g_{C_1C_3} = 8.0$ Å^{-1}, $h_{C_iH_j} = 1.4$ Å, and $h_{C_1C_3} = 1.9$ Å. The total potential energy V used in the trajectory studies is

$$V = V_{AM1} + V_{C_1C_3} + V_{C_1H_3} + V_{C_1H_4} + V_{C_3H_3} + V_{C_3H_4} \quad (3)$$

where V_{AM1} is the contribution from the AM1-SRP Hamiltonian.

After making appropriate changes to the MOPAC derivative routine DHCORE, the AM1-SRP first derivatives were calculated using the default Dewar−Liotard[30] package in MOPAC. The accuracy of the derivatives was checked against double-sided finite-difference (not available in MOPAC) and found comparable, with the Dewar−Liotard technique about 6 times faster. (To match the accuracy of finite-difference it is necessary to decrease the THROLD parameter in subroutine DERNVO. We used 0.0001.) To get the complete derivatives the AM1-SRP derivatives were combined with those obtained by differentiating eq 1.

Figure 1 shows the geometries of the stationary points located with AM1-SRP and Table 1 compares the relative energies of these stationary points with those obtained from *ab initio* results.[12] The character of the surface is similar to the *ab initio* PES. There is a shallow C_2 minimum **1** with a slight conrotatory rotation of the CH_2 groups, and a conrotatory cyclization saddle point **2**. The saddle point for single CH_2 rotation is **4** (C_s) and the saddle point for propylene formation is **6**. Figure 2 places **1**−**5** on a 2-dimensional PES defined by the torsion angles.

There are several differences from the *ab initio* PES. The AM1-SRP surface has no detectable C_s minimum with disrotatory CH_2 rotations, and the saddle point for disrotatory cyclization **5** is a second order saddle point with two negative eigenvalues of the second derivative matrix. With AM1-SRP the C_{2v} structure **3** (edge-to-edge or (0,0) trimethylene) is the saddle point for interconversion of enantiomeric structures **1**. On the *ab initio* surface the (0,0) C_{2v} structure is a second order saddle point.[27] *Ab initio* calculations predict **4** to have C_1 symmetry instead of the exact (0,90) conformation obtained from AM1-SRP, and the (0,90) C_s structure is a second order saddle point on the *ab initio* PES.[27] On the AM1-SRP surface the transition vector of **4** is about 2.5:1 $C_1H_1H_2$ rotation to $C_3H_5H_6$ rotation; on the *ab initio* PES it is nearly all $C_3H_5H_6$ rotation. Thus, the IRC path passing through **4** primarily involves a twist of a single CH_2 for both the AM1-SRP and *ab initio* potentials. However, for the former the path connects the two enantiomeric structures **1**, while for the latter it connects cis and trans cyclopropane. In Figure 2 the minimum energy path for cis−trans isomerization of cyclopropane is cis → **1** → **4** → **1′** → trans (labeled "cis−trans IRC"), where **1′** is the enantiomer of **1**. An alternative non-IRC path directly connects cis and trans cyclopropane via **4** and is less than 0.1 kcal mol^{-1} higher in energy. (Using the MOPAC Eigenvector following geometry search routine, we were unable to find any genuine saddle point for concerted cis−trans isomerization of cyclopropane or disrotatory cyclization of trimethylene.)

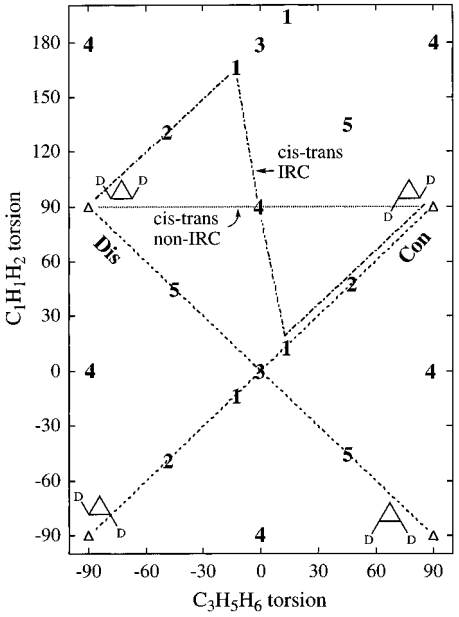

Figure 2. Location of stationary structures **1**−**5** on a 2-dimensional PES defined by the $C_1H_1H_2$ and $C_3H_5H_6$ torsion angles.

The middle of Figure 2, especially along the conrotatory path, is very flat with a total variation of 0.4 kcal mol^{-1} between enantiomeric structures **2**. As shown in Table 1, optical isomerization (enantiomeric interconversion) of cyclopropane via the conrotatory path is preferred over the disrotatory path by 2.2 kcal mol^{-1} with zero point energy (ZPE) correction. The ZPE-corrected barrier for cis−trans isomerization is 59.6 kcal

(30) Dewar, M. J. S.; Liotard, D. A. *J. Mol. Structure (Theochem)* **1990**, *206*, 123.

mol^{-1} (60−61 kcal mol^{-1} from experiment[28]), which is 5.0 kcal mol^{-1} less than the barrier for H-transfer; the experimental difference is 3.7 kcal mol^{-1}.[28]

III. The Direct Dynamics Procedure

A. Trajectory Initialization. The trajectories were initialized in two ways. The efficient microcanonical sampling scheme (EMS),[31] which takes anharmonic effects into account, was used to prepare microcanonical ensembles of the complete trimethylene classical phase space for total angular momentum $J = 0$ and total energies of 54.6, 77, 107, 146.4, and 164 kcal mol^{-1}. This spans the range of energies that were investigated in the previous variational RRKM calculation[12] and includes the energy−146.4 kcal mol^{-1}—at which experimental data are available.[7] To compare with the dynamics resulting from the EMS initialized trajectories, trimethylene was also excited nonrandomly at the same energies by using quasiclassical normal mode sampling[32] to initialize statistical distributions at the saddle point separating trimethylene and propylene. The total angular momentum is set to zero in both initialization procedures since, similarly to calculations of Doubleday,[12] we assume that the femtosecond laser experiments of Zewail's group yield a rotationally cold trimethylene intermediate. The agreement between Doubleday's calculated rate constants (at $J = 0$) and the experimental data supports this assumption. The details of the trajectory initialization and propagation are discussed in the final section of the paper.

B. Analysis of the Trajectory Results. 1. Definition of the Transition States. Working definitions of the cyclization and H-transfer transition states are required to determine the trimethylene lifetimes at various energies. The trimethylene−propylene transition state was assumed to be the same as the H-transfer saddle point and was not affected by a change in the energy. This assumption is consistent with the procedure used to initialize trajectories at the H-transfer transition state. The trimethylene−propylene saddle point is shown in Figure 1 and H-transfer occurs when either the C_2H_3 or C_2H_4 bond elongates and the C_1H_3, C_1H_4, C_3H_3, or C_3H_4 distance shortens accordingly.

The cyclization variational transition state is energy dependent and was defined in terms of the $C_1C_2C_3$ angle. The angle that is associated with the transition state at each preselected energy was determined from the EMS sampling scheme. The number of times that each $C_1C_2C_3$ angle was selected while performing this microcanonical sampling is proportional to the number of states associated with that angle. A minimum in the number of states corresponds to the variational transition state.[9,10,33] The presence of a fairly broad minimum at most of the energies made it difficult to unambiguously associate a single $C_1C_2C_3$ angle with the transition state. Consequently, a set of EMS initialized trajectories were propagated and lifetimes determined for different transition state (*i.e.*, $C_1C_2C_3$ angle) definitions. The angle that gave the fewest barrier recrossings was identified with the transition state. In fact, the precise definition of the $C_1C_2C_3$ angle—to within 2−3°—does not significantly affect the decay rate or the number of barrier recrossings (which is negligible at the energies studied). The cyclization transition state definitions obtained in this way are $C_1C_2C_3 = 94°$ at 54.6 kcal mol^{-1}, 92° at 77 kcal mol^{-1}, 90° at 107 kcal mol^{-1}, 89° at 146.4 kcal mol^{-1}, and 87° at 164 kcal mol^{-1}.

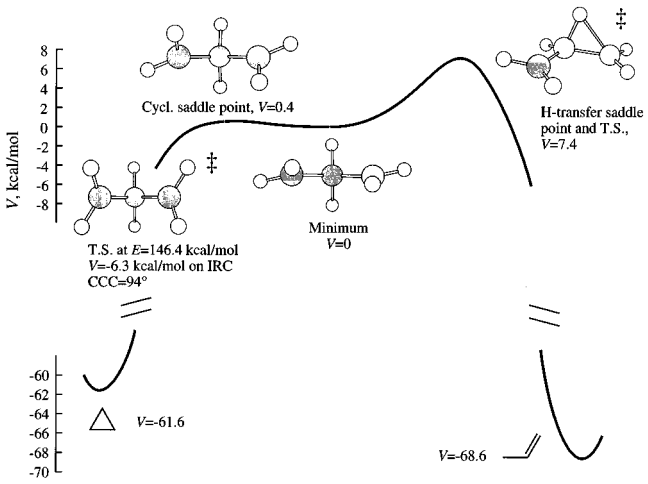

Figure 3. Minimum potential energy along the cyclopropane ↔ trimethylene ↔ propylene reaction path. The curve linking the stationary points merely serves to illustrate connectivity.

The relative potential energies for conrotatory cyclization and H-transfer are summarized in Figure 3, where the cyclization path includes the location of the variational transition state for 146.4 kcal mol^{-1} along the IRC for conrotatory cyclization. The curves linking the stationary points merely serve to illustrate the connectivity.

2. Unimolecular Rate Constants. RRKM theory assumes that the unimolecular decomposition is statistical with the probability that decomposition occurs in the time interval t to $t + dt$ given by the lifetime distribution

$$P(t) = -\frac{1}{N(0)}\frac{dN(t)}{dt} = ke^{-kt} \tag{4}$$

where k is the RRKM rate constant.[34] Thus, if trimethylene decomposition obeys the assumption that underlies RRKM theory, a single exponential lifetime distribution is expected whose intercept and exponential constant equal the RRKM rate constant.[35] Unless stated otherwise, the lifetime distributions presented here correspond to the first time trimethylene crosses the cyclization or H-transfer transition state. This allows for direct comparison of the rate constants extracted from the trajectory $P(t)$ plots with the RRKM rate constants, *i.e.*, RRKM theory assumes no recrossing at the transition state separating reactant from product. The total rate constant for trimethylene decay is

$$k_{tot} = k_{cycl} + k_{prop} \tag{5}$$

where k_{cycl} is the cyclization rate constant and k_{prop} is the H-transfer rate constant. The normalized branching ratio of cyclization to H-transfer is

$$k_{cycl}/k_{tot}:k_{prop}/k_{tot} \tag{6}$$

When a microcanonical statistical method is employed to initialize the trajectories the $t = 0$ intercept of $P(t)$ gives the anharmonic RRKM rate constant. The rate constant that is obtained when using (classical) EMS initialization is identified as k_{anh}^{cl}.

3. Power Spectra. The applicability of power spectral analysis to the understanding of intramolecular dynamics and

(31) Nyman, G.; Nordholm, S.; Schranz, H. W. *J. Chem. Phys.* **1990**, *93*, 6767.

(32) Chapman, S.; Bunker, D. L. *J. Chem. Phys.* **1975**, *62*, 2890. Sloane, C. S.; Hase, W. L. *J. Chem. Phys.* **1977**, *66*, 1523.

(33) Hase, W. L. *J. Chem. Phys.* **1976**, *64*, 2442. Truhlar, D. G.; Garrett, B. C. *Acc. Chem. Res.* **1980**, *13*, 440. Truhlar, D. G.; Hase, W. L.; Hynes, J. T. *J. Phys. Chem.* **1983**, *87*, 2664.

(34) Robinson, P. J.; Holbrook, K. A. *Unimolecular Reactions*; Wiley-Interscience: New York, 1972; Forst, W. *Theory of Unimolecular Reactions*; Academic Press: New York, 1973.

(35) Hase, W. L. In *Potential Energy Surfaces and Dynamics Calculations*; Truhlar, D. G., Ed.; Plenum: New York, 1979; p 1.

energy transfer pathways has been demonstrated previously.[36] The spectrum of a dynamic variable $q(t)$ is obtained from the Fourier transform

$$I(\nu) = \int_{-T}^{T} \mathrm{d}\tau\, C_{qq}(\tau) \mathrm{e}^{-2\pi i \nu \tau} \tag{7}$$

where $I(\nu)$ is the intensity at a frequency ν and T is the length of the trajectory that is propagated to obtain the autocorrelation function C_{qq}. This is given by

$$C_{qq}(\tau) = \lim_{T\to\infty} \frac{1}{T} \int_0^T \mathrm{d}t\, q(t) q(t+\tau) \tag{8}$$

A composite spectrum, pertaining to the motion of the entire trimethylene molecule, was obtained from the time development of all nine atomic coordinates. $C_{qq}(\tau)$ in eq 8 was calculated from trajectories followed for 2.5 ps which gives an $I(\nu)$ spectral resolution of 6.4 cm^{-1}.

IV. RRKM Calculations

The RRKM rate constant for a non-rotating molecule with an internal energy E may be expressed as

$$k(E) = \frac{N^{\ddagger}(E)}{h\rho(E)} \tag{9}$$

where $N^{\ddagger}(E)$ is the number of vibrational levels at the transition state and $\rho(E)$ is the reactant density of states.[34] Both classical and quantum harmonic RRKM rate constants were calculated to compare with the classical anharmonic RRKM rate constants that were determined from the trajectories. The Beyer−Swinehart algorithm[37] was used to obtain the quantum harmonic $N^{\ddagger}(E)$ and $\rho(E)$ in eq 9. The classical harmonic RRKM rate constant is given by

$$k_{\mathrm{har}}^{\mathrm{cl}}(E) = \frac{\prod_{i=1}^{s} \nu_i}{\prod_{i=1}^{s-1} \nu_i^{\ddagger}} \left[\frac{E - E_0}{E}\right]^{s-1} \tag{10}$$

where the ν_i and $\nu_i^{\ddagger}$ are the reactant and transition state harmonic vibrational frequencies, respectively, and E_0 is the potential energy difference between the transition state and reactant, neglecting zero point energy. The trimethylene harmonic vibrational frequencies are 59, 262, 422, 648, 695, 798, 946, 1006, 1044, 1184, 1225, 1382, 1389, 1433, 1512, 3101, 3134, 3242, 3244, 3256, and 3256 cm^{-1}.

The H-transfer transition state is assumed to be energy independent and is located at the trimethylene ↔ propylene saddle point. Its harmonic vibrational frequencies are 313, 419, 468, 744, 787, 896, 938, 1034, 1182, 1238, 1333, 1394, 1441, 1610, 2858, 3165, 3234, 3238, 3252, and 3255 cm^{-1}, and its classical barrier height, E_0, is 7.35 kcal mol^{-1}.

Variational RRKM theory was used to determine the energy dependent cyclization transition state structures. An intrinsic reaction path was determined by following the path of steepest descent in mass-weighted Cartesian coordinates, and harmonic frequencies for the modes orthogonal to the reaction coordinate were calculated at each point along the path.[38] The transition state at a specified energy is the configuration which corresponds to a minimum in $N^{\ddagger}(E)$ along the path.[9,10,33] This procedure is followed for both the conrotatory and disrotatory cyclization paths. Even though the disrotatory path passes over a second-order saddle point, there is only one imaginary frequency in the region of the variational transition state, which occurs ≈1 kcal/mol below **5** in Figure 1. In the quantum RRKM calculations the $C_1C_2C_3$ angle of the variational transition state at 54.6 kcal mol^{-1} is $C_1C_2C_3 = 106.5°$ along the conrotatory path and 104.6° along the disrotatory path. At 164 kcal mol^{-1} these values decrease to 97.45° and 93.68°, respectively. The corresponding classical transition states at 54.6 kcal mol^{-1} are at 105.5° along the conrotatory path and 103.3° along the disrotatory path while at 164 kcal mol^{-1} they occur at 96.8° and 93.3°, respectively. Clearly, the location of the transition states is fairly insensitive as to whether the quantum or classical $N^{\ddagger}(E)$ is being minimized. However, the omission of anharmonic effects yields transition state structures with larger $C_1C_2C_3$ angles than those obtained from the EMS sampling which includes anharmonicity. The latter gives an angle of 94° and 87° at 54.6 and 164 kcal mol^{-1}, respectively, for the conrotatory path.

The CH_2 torsional modes of trimethylene have low frequencies (*i.e.*, 59 and 262 cm^{-1}) and at high energies it may be more accurate to treat these modes as free rotors instead of harmonic oscillators.[39] This was done in a second set of RRKM calculations. The free rotor approximation was not applied to the cyclization and H-transfer transition states since the torsional modes have stiffened and, accordingly, their frequencies have increased substantially. A standard RRKM computer package was used to determine the classical and quantum harmonic rate constants.[40]

The harmonic RRKM rate constants and product branching ratios are listed in Table 2. The total rate constant k_{tot} is a sum of k_{con}, k_{dis}, and k_{prop} computed by variational location of the transition states for cyclization (along the con and dis IRC paths) and propene formation. The classical and quantum rate constants and branching ratios are in good agreement, especially at high energies. When the trimethylene torsional modes are treated as free rotors, instead of harmonic oscillators, the rate constant is smaller at low energies and larger at high energies. This is the expected trend since at low to moderate energies the free rotor approximation will lead to a higher density of states than the harmonic oscillator approximation (rotational states are generally more dense than vibrational states). Since the free rotor density of states increases as $E^{0.5}$ whereas the harmonic oscillator density of states increases as E,[39] the density of free rotor states is lower than the density of vibrator states at elevated energies.

V. Trajectory Results

A. EMS Initialization. When the EMS scheme is used to excite trimethylene at 54.6 and 77 kcal mol^{-1} the lifetime distribution $P(t)$ is biexponential. This is shown in Figure 4 for the lower energy and indicates a decoupling of reactant phase space such that, within the time scale of reaction, the system is non-ergodic. The decomposition is thus intrinsically non-

(36) Bendat, J. S.; Piersol, A. G. *Engineering applications of correlation and spectral analysis*; Wiley: New York, 1980. Sewell, T. D.; Thompson, D. L.; Levine, R. D. *J. Phys. Chem.* **1992**, *96*, 8006. Sewell, T. D.; Chambers, C. C.; Thompson, D. L.; Levine, R. D. *Chem. Phys. Lett.* **1993**, *208*, 125.

(37) Gilbert, R. G.; Smith, S. C. *Theory of Unimolecular and Recombination Reactions*; Blackwell Scientific Publications: Oxford, 1990.

(38) Truhlar, D. G.; Kupperman, A. *J. Am. Chem. Soc.* **1971**, *93*, 1840. Truhlar, D. G.; Kupperman, A. *J. Chem. Phys.* **1972**, *56*, 2232. Miller, W. H.; Handy, N. C.; Adams, J. E. *J. Chem. Phys.* **1980**, *72*, 99. Isaacson, A. D.; Truhlar, D. G. *J. Chem. Phys.* **1985**, *76*, 1380. Hase, W. L.; Duchovic, R. J. *J. Chem. Phys.* **1985**, *83*, 3448. Vande Linde, S. R.; Mondro, S. L.; Hase, W. L. *J. Chem. Phys.* **1987**, *86*, 1348.

(39) Davidson, N. *Statistical Mechanics*; McGraw-Hill: New York, 1962.

(40) Zhu, L.; Hase, W. L. *QCPE* **1995**, *14*, 644.

Table 2. Classical and Quantum RRKM Harmonic Rate Constants (ps^{-1}) for the Decomposition of Trimethylene[a]

energy[b]	k_{con}	k_{dis}	k_{prop}	k_{tot}	k_{cycl} / k_{tot}:k_{prop} / k_{tot}
			Classical		
54.6	1.29 (1.10)	3.04 (2.60)	0.26 (0.22)	4.59 (3.92)	0.94:0.06 (0.94:0.06)
77	1.29 (1.54)	3.22 (3.84)	0.62 (0.74)	5.13 (6.12)	0.88:0.12 (0.88:0.12)
107	1.25 (2.07)	3.03 (5.03)	1.12 (1.85)	5.40 (8.95)	0.79:0.21 (0.79:0.21)
146.4	1.16 (2.63)	2.56 (5.81)	1.64 (3.74)	5.36 (12.18)	0.69:0.31 (0.69:0.31)
164	1.11 (2.82)	2.34 (5.96)	1.86 (4.71)	5.31 (13.49)	0.65:0.35 (0.65:0.35)
			Quantum		
54.6	1.18 (0.60)	2.08 (0.99)	0.01 (0.00)	3.27 (1.59)	1.00:0.00 (1.00:0.00)
77	1.29 (1.25)	3.11 (3.01)	0.39 (0.37)	4.79 (4.63)	0.92:0.08 (0.92:0.08)
107	1.25 (1.89)	3.07 (4.64)	0.98 (1.47)	5.30 (8.00)	0.81:0.19 (0.82:0.18)
146.4	1.17 (2.53)	2.62 (5.67)	1.58 (3.40)	5.37 (11.60)	0.71:0.29 (0.71:0.29)
164	1.12 (2.76)	2.39 (5.88)	1.80 (4.40)	5.31 (13.04)	0.66:0.34 (0.66:0.34)

[a] This is the normalized branching ratio as given in eq 6. The rate constants obtained when employing a free rotor approximation for the two CH_2 torsional modes of trimethylene are presented in parentheses. [b] Energy is in kcal mol^{-1}.

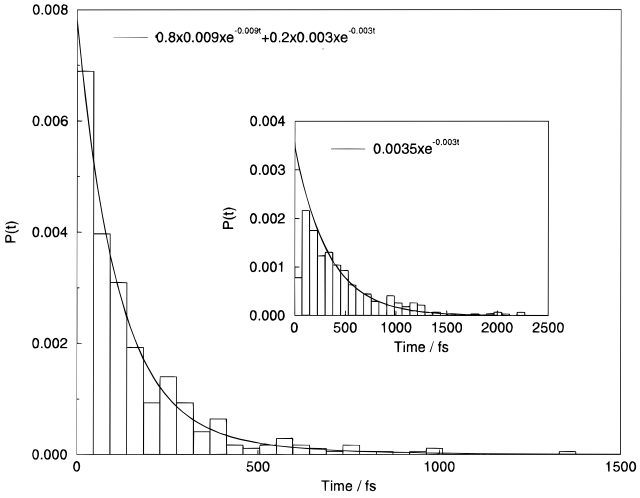

Figure 4. Lifetime distribution of the trimethylene biradical at 54.6 kcal mol^{-1} when the trajectories are initialized using the EMS scheme. The double exponential shape of the decay curve reveals that the decay is non-statistical at this energy. The initial decay rate, k_{anh}, is $\approx$7 ps^{-1} whereas the rates associated with the double exponential are 9 and 3 ps^{-1}. The inset shows the corresponding plot when the trajectories are initialized at the trimethylene−propylene barrier. Although the decay is single exponential, it decays with a rate of 3 ps^{-1} which is slower than k_{anh}. The sensitivity of the decay dynamics to the initialization scheme employed is a feature of non-ergodic systems.

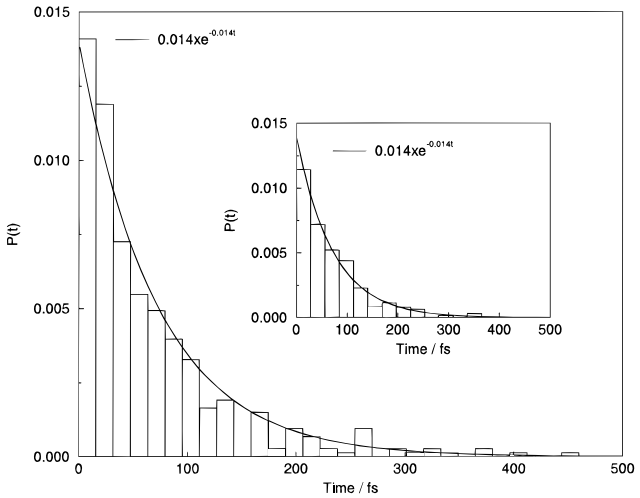

Figure 5. Same as for Figure 1 but at an energy of 146.4 kcal mol^{-1}. The insensitivity of the decay dynamics to the initialization scheme and the fact that the single exponential decay rate is the same as k_{anh} (14 ps^{-1}) shows that the decay is statistical at this energy.

RRKM[35,41] with only the intercept of $P(t)$ equal to the anharmonic microcanonical RRKM rate constant. At 107 and 146.4 kcal mol^{-1} the trajectories exhibit single exponential decay with a rate constant that equals the intercept of $P(t)$. Thus, at these energies the decomposition is intrinsically RRKM. The lifetime distribution obtained at 146.4 kcal mol^{-1} is illustrated in Figure 5. Biexponential decay is observed again at 164 kcal mol^{-1}. In contrast to the biexponential behavior at low energies, it is associated with the dynamics of high-energy reactions;[42] that is, a large percentage ($\approx$40−50%) of the trajectories decay within one vibrational period of the cyclization or H-transfer reaction coordinate. The top half of Table 3 summarizes the properties of the lifetime distributions following EMS initialization.

Cyclization transition state recrossings do not significantly affect the rate constants at any of the energies. Also, at low energies—54.6, 77, and 107 kcal mol^{-1}—recrossings of the H-transfer barrier do not have a large effect on the decay rate. When determining H-transfer rate constants from the final time

Table 3. Characteristics, Rate Constants, and Product Branching Ratios from Trajectory Simulations of Trimethylene Decomposition[a]

energy	fit to $P(t)$	rate constant(s)[b]	k_{anh}^{cl} [c]	branching ratio[d]
		EMS Initialization		
54.6	double exp.	9 (80%), 3 (20%)	7	0.90:0.10
77	double exp.	11 (85%), 3 (15%)	8	0.73:0.27
107	single exp.	10	10	0.60:0.40
146.4	single exp.	14	14	0.51:0.49
164	double exp.	30 (70%), 7 (30%)	18	0.49:0.51
		Barrier Initialization[e]		
54.6	single exp.	3		0.84:0.16
77	double exp.	7 (60%), 4 (40%)		0.68:0.32
107	single exp.	9		0.58:0.42
146.4	single exp.	12		0.49:0.51
164	double exp.	20 (70%), 7 (30%)		0.41:0.59

[a] The energy is in kcal mol^{-1} and the rate constant, determined from the first passage through the transition states, is in ps^{-1}. [b] For biexponential decay the percentage of trajectories decaying with a certain rate constant is given in parentheses. [c] The intercept of $P(t)$ following EMS initialization. [d] [Number of trajectories forming cyclopropane/total number of reacted trajectories]:[number of trajectories forming propylene/total number of reacted trajectories]. [e] For barrier initialization reaction is initially suppressed; see Figure 4. However, all of $P(t)$ was still fit by a single or double exponential.

trimethylene crosses the barrier at 54.6 kcal mol^{-1}, the decay is double exponential with 70% of the trajectories reacting with a rate constant of 9 ps^{-1} and 30% with a rate constant of 3 ps^{-1}. This is similar to the double exponential decay observed when recrossings were not taken into account (80% decayed at

(41) Bunker, D. L.; Hase, W. L. *J. Chem. Phys.* **1973**, *59*, 4621.
(42) Bolton, K.; Nordholm, S.; Schranz, H. W. *J. Phys. Chem.* **1995**, *99*, 2477.

9 ps^{-1} and 20% at 3 ps^{-1}). At 107 kcal mol^{-1} the decay remains single exponential when recrossings are taken into account and there is a slight decrease in the rate from 10 to 8.5 ps^{-1}. At higher energies the effect of recrossings becomes more severe. At 146.4 kcal mol^{-1} the rate constant decreases from 14 to 11 ps^{-1} when including the effect of recrossings while the decay remains single exponential. At 164 kcal mol^{-1} the double exponential decay shows that 70% of the trajectories decay with a rate of 20 ps^{-1} and 30% with a rate of 7 ps^{-1} when recrossings are accounted for. Comparison with the data in Table 3 shows that the decrease in decay rate is primarily due to recrossings of the rapidly decaying trajectories.

A comparison of the classical anharmonic microcanonical (*i.e.*, RRKM) rate constants determined from the $P(t)$ intercept, and listed in Table 3, with the classical harmonic RRKM rate constants listed in Table 2 shows reasonable agreement at all energies studied. At 54.6 kcal mol^{-1}, where the agreement is poorest, the anharmonic RRKM rate constant ($\approx$7 ps^{-1}) and the harmonic RRKM predictions obtained from both the harmonic oscillator approximation (4.59 ps^{-1}) and the free rotor approximation for the torsions (3.62 ps^{-1}) are of the same magnitude. The free rotor is expected to become more accurate as the energy is increased and at 146.4 kcal mol^{-1}, where the decay is intrinsically RRKM, the anharmonic rate constant of $\approx$14 ps^{-1} is in agreement with the harmonic prediction of 12.18 ps^{-1} obtained with the free rotor approximation.

Usually anharmonicity increases the reactant density of states ρ(E) in eq 9 to decrease the RRKM rate constant.[43] Thus, it was somewhat surprising to find the harmonic RRKM are constants smaller than the anharmonic values. A possible origin of this effect would be quartic anharmonicity for the trimethylene CH_2 wags, as is the case for the CH_3 radical,[44] which would decrease the density of states. However, an investigation of the potentials for the trimethylene CH_2 wags showed them to be quite harmonic. A complete understanding of the difference between the harmonic and anharmonic RRKM rate constants for trimethylene may require an accurate calculation of the anharmonic sums $N^{\ddagger}(E)$ and the density of states $\rho(E)$, as has been done for other unimolecular reactions.[45]

B. Barrier Initialization. A prominent feature of the lifetime distribution when the trajectories are initialized at the trimethylene−propylene barrier is the smaller initial decay rates compared to those for the EMS initialization. This is illustrated for the energy of 54.6 kcal mol^{-1} in the inset to Figure 4. The shortest lifetime associated with cyclization is $\approx$80 fs and, thus, the vast majority of the trajectories that decay in the initial 80 fs time period form propylene. This initial rate for propylene formation is not significantly different from that found from EMS initialization (*i.e.*, see rate constants and branching ratios in Table 3). Thus, the principal effect on the decay, when initializing trajectories at the trimethylene−propylene barrier and thus exciting trimethylene non-randomly, is to initially suppress cyclization. This is an apparent non-RRKM effect arising from the non-random sampling of phase space.[35,41] However, this initial non-random decomposition has a minor effect on the overall product branching ratios which, as shown in Table 3, are quite similar for EMS and barrier initialization.

The lower half of Table 3 lists the decay results and branching ratios obtained when the trajectories were initialized at the barrier. Though, as shown in Figure 5, reaction is initially suppressed, the lifetime distributions were still fit by single and double exponentials which give a good representation of the $P(t)$ except for the initial decay. At 54.6 kcal mol^{-1} the fitted $P(t)$ is single exponential with a rate constant equal to the long-time component of $P(t)$ for EMS initialization. The phase space dynamics of the trajectories initialized at the barrier may be similar to those which contribute to the slow exponential decay component of $P(t)$ following EMS initialization.

At 77 kcal mol^{-1} $P(t)$ is double exponential as for the EMS initialized trajectories. However, the relative contributions of the fast and slow decays are different, as are their rate constants. These results are consistent with non-ergodic dynamics and intrinsic non-RRKM kinetics at this energy. At 107, 146.4, and 164 kcal mol^{-1} the lifetime distributions for the barrier and EMS initialized trajectories are nearly the same. The lifetime distribution at 146.4 kcal mol^{-1} is illustrated in the inset to Figure 5. The decay is single exponential and decays with a rate that equals the anharmonic microcanonical decay rate. The decay behavior is independent of the method of initialization and, since the cyclization:H-transfer branching ratio is also the same for both types of initialization (see Table 3), it indicates that all of the trajectories that are started at the trimethylene−propylene barrier are trapped in trimethylene phase space before crossing either the trimethylene−cyclopropane or trimethylene−propylene barrier. This insensitivity to the initialization procedure is a feature of ergodic systems. The same type of behavior is observed at 107 kcal mol^{-1}.

The double exponential decay seen at 164 kcal mol^{-1} was discussed above; *i.e.*, it is due to the extremely rapid decay of a significant proportion of trajectories—often within one vibrational period of the reaction coordinate. The effect of barrier recrossings on the lifetime distribution decay is similar to that observed for EMS initialized trajectories; the effect increases at elevated energies so that substantial decreases in the decay rates are seen at 146.4 and 164 kcal mol^{-1}.

C. Quasiclassical Trajectories and Power Spectra. Trajectories were initialized near the trimethylene potential minimum with quasiclassical normal mode sampling[32] to study the non-ergodic dynamics at 54.6 kcal mol^{-1} in more detail. Trajectories were chosen such that all modes had zero point energy. The excess energy of $\approx$7 kcal mol^{-1} was distributed in two different ways. In the first it was distributed between the five lowest frequency modes so that modes 1, 2, 4, and 5 (in order of increasing frequency) had one quantum each (above zero point energy) and mode 3 had two quanta. This energy distribution gave the required total energy of 54.6 kcal mol^{-1}. Second, all of the excess energy was initially put in the lowest frequency mode. Figure 6 is a typical power spectrum obtained from 2.5 ps of internal motion when the excess energy was distributed among the five low-frequency modes. The structured appearance of the spectrum indicates that the trimethylene dynamics is not ergodic. The decay associated with these trajectories (see the stars in the inset of Figure 6) is significantly slower than the decay obtained when all of the excess energy was placed in the lowest frequency mode (see the circles in the inset). For the former the decay is slower than that for EMS initialization while for the latter it is faster, *i.e.*, compare Figures 4 and 6. The regular structure of the power spectrum and the dependence of the long-time features of the lifetime distribution on the mode(s) excited are indicative of decoupled intramolecular dynamics on the time scale of the reaction.

VI. Comparison to Experiment

In this section the trajectory results obtained at 146.4 kcal mol^{-1} for rotationally cold trimethylene are compared with the

(43) Baer, T.; Hase, W. L. *Unimolecular Reaction Dynamics: Theory and Experiments*; Oxford University Press: New York, 1996.

(44) Duchovic, R. J.; Hase, W. L.; Schlegel, H. B. *J. Phys. Chem.* **1984**, *88*, 1339.

(45) Peslherbe, G. H.; Hase, W. L. *J. Chem. Phys.* **1994**, *101*, 8535. Peslherbe, G. H.; Wang, H.; Hase, W. L. *J. Chem. Phys.* **1995**, *102*, 5626.

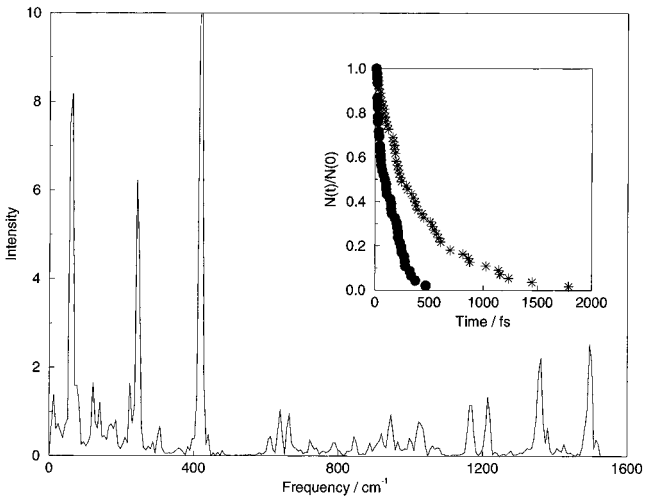

Figure 6. A typical power spectrum of the trimethylene dynamics at 54.6 kcal mol^{-1} when all vibrational modes initially have zero point energy and the remaining energy (7 kcal mol^{-1}) is partitioned between the five lowest frequency modes. Only those peaks below 1600 cm^{-1} are shown for the sake of clarity. The structured appearance of the spectrum shows that the trimethylene dynamics is regular at this energy. The inset illustrates the significantly different decay rates obtained when initializing the trajectories in this way (stars) and when the remaining energy is initially in the lowest frequency mode (circles).

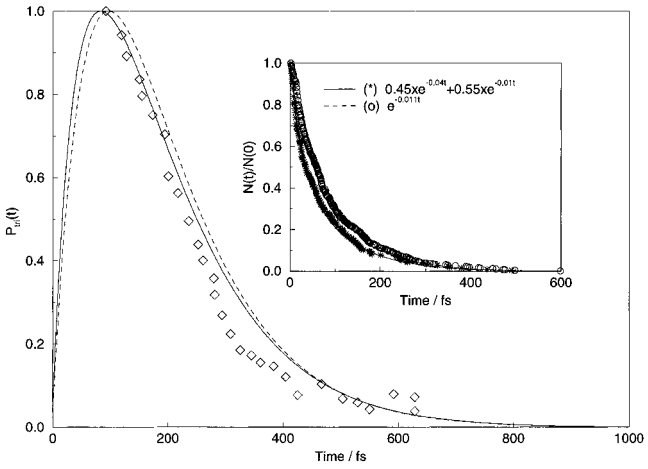

Figure 7. Comparison of the simulated decay rates at 146.4 kcal mol^{-1} with the experimental data obtained from ref 7 (diamonds). The curves are obtained when the effects of the finite trimethylene risetime are taken into account (see text). The solid curve corresponds to the double exponential decay observed when the trajectories are initially in an approximate face-to-face configuration (the decay is shown by the stars in the inset) and the dashed curve corresponds to the single exponential decay observed when EMS initialization is employed (the decay is shown by the circles in the inset).

femtosecond laser experiment of Pedersen *et al.*[7] where an isolated, rotationally cold cyclobutanone molecule is laser excited to induce fragmentation to CO and trimethylene. The trimethylene photofragment has an energy of ≈99 kcal mol^{-1} (in excess of the zero point energy) which corresponds to our trajectory energy of 146.4 kcal mol^{-1}. The features of the potential surface on which the photofragments separate affect the vibrational, rotational, and translation energy of the trimethylene (and CO) molecule. For example, an anisotropic surface may lead to overall rotation of the trimethylene radical even though the parent molecule was rotationally cold. When comparing the trajectory results to the experimental data is is assumed that either the trimethylene is rotationally cold or that any possible rotation will have an insignificant effect on the intramolecular dynamics and decay. Since the trajectory dynamics of the non-rotating molecule is ergodic at this energy, rotations are not expected to effect the intramolecular vibrational energy transfer (rotations usually enhance IVR). However, rotations may affect the RRKM rate constant.

The initial configurations and modes excited for trimethylene prepared by cyclobutanone photodissociation depend on the features of the cyclobutanone potential surface. In cyclobutanone the trimethylene has an approximate face-to-face structure. If the departing CO fragment has no affect on this configuration then the trimethylene photofragment will initially maintain the face-to-face structure. Alternatively, if the departing CO induces rotation of the terminal CH_2 groups then the structures of the trimethylene photofragments may be well represented by the configurations obtained by statistical sampling schemes, *e.g.*, EMS.

The effect of initializing the trajectories in an approximate face-to-face configuration was studied with the EMS scheme by only accepting configurations where the terminal torsions were between 85 and 95°. The subsequent decay—obtained from the final time of barrier crossing—was double exponential with 45% of the trajectories decaying with a rate of ≈40 ps^{-1} and 55% decaying with a rate of ≈10 ps^{-1}. The initial rapid decay is primarily due to trajectories that cyclize extremely quickly (sometimes directly) as a result of the unpaired p-orbital electrons initially having the correct orientation for ring closure. For EMS sampling, without constraining the torsions, the decay obtained from the final time of barrier crossing is exponential with a rate constant of 11 ps^{-1}. This rate is nearly the same as 8.3 ± 1.4 ps^{-1} measured by Pedersen et al.[7]

The inset to Figure 7 shows the decay at 146.4 kcal mol^{-1} when trimethylene is excited non-randomly with the torsions initially constrained between 85° and 95° (stars) is similar to that when trimethylene is excited randomly with EMS initialization (circles). To facilitate comparison with the experimental data these decays are obtained from the final time that the trimethylene crosses either the cyclization or H-transfer barrier. The initial rapid decay of some of the trimethylene molecules that are in the face-to-face configuration is clearly evident. The experiment measures trimethylene versus time and to compare with experiment the rate of trimethylene formation from cyclobutanone must also be considered. The experimentally determined normalized number of excited cyclobutanone molecules versus time is exp(−t/105) and thus the probability for trimethylene formation by photodissociation at time $t = \tau$ is

$$P_{\text{form}}(\tau) = 1 - \exp(-\tau/105) \tag{11}$$

The number of trimethylene molecules versus time is then a convolution of this formation probability and the lifetime distribution determined from the trajectories, *i.e.*,

$$P_{\text{tri}}(t) = \int_0^t P_{\text{form}}(\tau) P(t-\tau)\, \mathrm{d}\tau \tag{12}$$

The normalized results are shown in Figure 7. The solid curve corresponds to the trajectories that initially have constrained torsions (and a double exponential decay) while the dashed curve corresponds to the EMS initialized trajectories. The experimental data are taken from Figure 4B of ref 7 and are shown as diamonds.

The simulated data obtained with the torsions initially constrained are in better agreement with the experimental data than the data obtained with trimethylene configurations sampled statistically. This indicates that there may not be a statistical sampling of trimethylene phase space before the photofragment reacts, *i.e.*, the initial face-to-face configuration of the trimeth-

ylene moiety in the parent cyclobutanone influences the subsequent dynamics of the trimethylene fragment. However, the similarity of both decay curves and the experimental results does not allow for definitive conclusions regarding the trimethylene dynamics and decay that occurs under the experimental conditions. A similar observation was made in ref 7 where it was noted that the trimethylene decay was not readily fitted by a single exponential.

VII. Conclusion

The simulations reported here of trimethylene decomposition illustrate the feasibility and computational affordability of direct trajectory methods when investigating systems of this size. Semiempirical evaluation of the internuclear forces allows for the explicit treatment of all degrees of freedom. Furthermore, direct trajectory techniques avoid the need to develop an analytic potential surface and consequently circumvent the approximations and assumptions associated with this approach. There is good agreement between the simulations and femtosecond laser experiments, which suggests that the semiempirical potential energy surface and trajectory calculations provide a valid description of the decomposition.

The simulations show that the intramolecular dynamics is non-ergodic at low energies and that the decay is intrinsically non-RRKM. This behavior is also observed when simulating quasiclassical trajectories and is thus not an "unphysical" result associated with the classical sampling scheme. At increased energies the lifetime distribution is single exponential with an exponential constant that equals the anharmonic RRKM rate constant. At very high energies a significant fraction of trajectories decay directly thereby leading to biexponential decay.

For low energies the harmonic RRKM rate constant is approximately 50% smaller than the anharmonic RRKM rate constant obtained from the EMS initialized trajectories. The difference decreases and approaches 10% at the higher energies. Treating the two CH_2 torsions of trimethylene as free rotors, instead of harmonic oscillators, seems to be a more accurate representation at elevated energies. A rigorous treatment of anharmonic effects is required in order to obtain RRKM predicted rate constants that are valid at all energies.

VIII. Computational Section

A. Trajectory Initialization. 1. EMS Initialization. The EMS scheme for preselected total angular momentum, discussed in detail elsewhere,[31] was modified slightly for the present application. The AM1-SRP barrier for internal rotation of a trimethylene terminal CH_2 group is 2.0 kcal mol^{-1}. At the lowest energy studied the average energy in a single mode (54.6/21 = 2.6 kcal mol^{-1}) is of the same magnitude as the torsional barrier so that many Markov chain steps were required for multiple crossings of the barrier (which is necessary for a complete sampling of the trimethylene phase space). It was important to ensure that the initial conditions of the trajectories comprising an ensemble represented a global sampling of reactant phase space. There are a number of ways to achieve this: One may perform many (5 to 10 million) steps along the Markov chain between each trajectory. However, since the energy at each trial state is determined semiempirically, this method is extremely inefficient. One may also increase the size of the steps along the chain in order to sample configurations corresponding to different potential minima more easily. For the trimethylene system the required step size (at 54.6 kcal mol^{-1} when a single coordinate is perturbed at each step) allows for only 10−20% acceptance of the trial configurations hence making this approach inefficient. One may also begin the Markov at different points in reactant phase space (*i.e.*, not just at the potential minimum). This was the approach adopted here. After every fifth trajectory the CH_2 terminals were rotated by a random amount between 0 and 360°. The new (trial) configuration was accepted or rejected according to the usual EMS procedures.[31] Since these torsional "kicks" are outside of the conventional EMS scheme, 10 000 "meltdown" steps were allowed after each kick so that any memory of the kick would be lost. [This meltdown period is equivalent to the meltdown that is found at the beginning of the conventional EMS scheme in order to lose the memory of the initial minimum energy configuration.]

This modification allowed for multiple crossings of the torsional barriers and statistical convergence that is more rapid than when the unmodified EMS scheme is employed. As expected, the converged results obtained from the modified procedure agree with the corresponding results obtained from the unmodified scheme (when in excess of 10 million steps are included in the Markov chain).

2. Initialization at the H-Transfer Barrier. The procedure for initialization at the trimethylene−propylene barrier selects the initial trajectory conditions according to a quasiclassical microcanonical statistical sampling of the normal mode vibrational states at the barrier. This procedure yields the quasiclassical analogue of the quantum harmonic statistical distribution at the barrier. Each quasiclassical normal mode state with energy E_j less than or equal to the microcanonical trajectory energy, E_{traj}, will have an equal probability of being selected. The excess energy, $E_{traj} - E_j$, is placed in the reaction coordinate so as to propel the reaction toward the trimethylene phase space.

The procedure for quasiclassical barrier sampling is based on the corresponding method for classical barrier sampling.[46] A normal mode i, which is orthogonal to the reaction coordinate, is randomly and uniformly selected and, using a relevant weighting procedure, randomly assigned an energy $E_i = (n_i + {}^1/_2)\hbar\omega_i$ such that $E_i \le E_{traj}$. The probability of assigning n_i quanta to this mode is

$$P(n_i) = W_{n_i}/W_{tot} \tag{13}$$

where W_{n_i} is the number of quasiclassical states with energy less than E_{traj} and with mode i having n_i quanta. This is determined by the Beyer−Swinehart algorithm.[37] W_{tot} is the normalization constant and is the sum of all possible states with energy less than or equal to E_{traj}, *i.e.*, $W_{tot} = \sum_{i=0}^{\infty} W_{n_i}$.

Once n_i quanta (or energy $(n_i + {}^1/_2)\hbar\omega_i$) has been assigned to mode i, the remaining energy, $E_{traj} - E_i$, is distributed among the other normal modes in a similar manner. Hence a second mode l is randomly chosen and assigned n_l quanta such that $E_l \le E_{traj} - E_i$. The probability of choosing n_l is

$$P(n_l) = W_{n_l}/W_{tot} \tag{14}$$

where W_{n_l} and W_{tot} are determined by the Beyer−Swinehart algorithm.

In general, after m normal modes have been assigned quanta $n_1,n_2,...,n_m$, mode $m+1$ is randomly chosen such that $m+1 \neq 1,2,...,m$. It is assigned n_{m+1} quanta such that

$$E_{m+1} \le E_{traj} - \sum_{i=1}^{m}\left(n_i + \frac{1}{2}\right)\hbar\omega_i \tag{15}$$

The probability of selecting n_{m+1} quanta is the same as that described above for modes i and l.

This procedure selects each state with equal probability and the momentum distribution in the reaction coordinate is consequently in agreement with RRKM theory.[37,34,43] The minimum energy (relative to the trimethylene minimum) that is allowed for this sampling scheme is the sum of the quasiclassical transition state zero point energy and the barrier height. At the trimethylene−propylene barrier this is 54.3 kcal mol^{-1}. An additional 0.3 kcal mol^{-1} was added in our lowest energy trajectories in order to propel the trajectories toward trimethylene phase space.

The Cartesian coordinates and momenta are obtained from the displacement of the (energized) normal modes from equilibrium.[47] Random phases are selected for the normal mode momenta and

(46) Hase, W. L.; Buckowski, D. G. *Chem. Phys. Lett.* **1980**, *74*, 284.
(47) Wilson, E. B., Jr.; Decius, J. C.; Cross, P. C. *Molecular Vibrations*; McGraw-Hill: New York, 1955.

coordinates.[32] Since the transformation of normal modes to Cartesian coordinates is not exact at elevated energies, it is necessary to scale the selected coordinates and momenta to obtain the desired microcanonical (trajectory) energy. The scaling factor is $(E_{traj}/E_{scale})^{1/2}$ where E_{traj} is the desired energy and E_{scale} is the energy determined from the coordinates and momenta which are being scaled.[22] The scaling is repeated in an iterative manner until the energy is within 0.1% of the desired value. Before the first scaling the magnitude of the difference between E_{scale} and E_{traj} was on average 4 and 14% of E_{traj} for the lowest and highest total energies, respectively (*i.e.*, 54.6 and 164 kcal mol^{-1}).

B. Trajectory Integration. The atomic motion is evaluated in the traditional classical trajectory fashion, as implemented by VENUS,[22] by solving Hamilton's equations with a combined fourth-order Runge−Kutta and sixth-order Adams−Moulton predictor−corrector integration algorithm.[48] At each step of the integration the Schrödinger equation is solved for electronic energies and forces on the nuclei by invoking the appropriate routines in MOPAC 7.0.[23] Once a converged SCF has been obtained and the configuration interaction has been included, the first derivatives of the energy with respect to the Cartesian positions are evaluated analytically within MOPAC 7.0. The starting point of the SCF calculation is taken to be the set of molecular orbital coefficients from the previous trajectory step and thus if the geometry is changing smoothly over time only 9 or 10 SCF iterations are necessary at each point.

(48) Bunker, D. L. *Meth. Comput. Phys.* **1971**, *10*, 287. Press, W. H.; Teukolsky, S. A.; Vetterling, W. T.; Flannery, B. P. *Numerical Recipes in Fortran*; *The art of scientific computing*; University Press: Cambridge, 1992.

Trajectories were integrated with a step size of 0.25 fs. Energy was conserved to four significant figures over the lengths of the trajectories studied (ranging up to 2.5 ps). The integration of a typical 200 fs trajectory required ≈788 cpu seconds on an IBM RS6000/370. The trajectories were propagated until either the cyclization transition state or the saddle point separating trimethylene and propylene was crossed. All of the trajectories that were initialized at the H-transfer barrier or using the EMS scheme reacted within the maximum time limit of 2.5 ps. The criterion for terminating the trajectory at the cyclopropane product was the $C_1C_2C_3$ angle decreasing to 75° (see Figure 1). This is at least 12° smaller than the angle at the cyclization transition state and allowed assessment of barrier recrossings. The criterion for terminating the trajectories that yield propylene was that the C_2H_3 or C_2H_4 bond was at least 2.3 Å and the corresponding C_1H_3, C_1H_4, C_3H_3, or C_3H_4 distance was shorter than 1.3 Å. These configurations lie on the propylene side of the H-transfer barrier (see Figure 1) and using them as a criterion for terminating the trajectories facilitated evaluating the effects of recrossing the trimethylene−propylene saddle point.

Acknowledgment. K.B., G.P., and W.L.H. are grateful for financial support from the National Science Foundation, CHE-94-03780. C.D. is grateful for financial support from the National Science Foundation, CHE-94-20826.

JA962434T